# The electronic structure and optical properties of $CsAX_2X'$ (A=Ge, Sn, Pb; X, X'=Cl, Br, I) Halide perovskites

GUANGTAO WANG[a,*], JUNHONG WEI[a,b], DONGYANG WANG[a], YUFENG PENG[a]
[a]*College of Physics and Electronic Engineering, Henan Normal University, Xinxiang, Henan 453007, China*
[b]*School of Mechanical and Electrical Engineering, Henan Institute of Science and Technology, Xinxiang, Henan 453003, China*

The crystal structures, electronic structures and optical properties of mixed halides perovskites $CsAX_2X'$ (A=Ge, Sn, Pb; X, X'=Cl, Br, I) compounds are studied by the first-principle calculations. Band structure calculations, with mBJ+SOC (modified Beak Johnson approximation plus spin-orbit coupling) method, indicate that these compounds are semiconductors with the direct band gap ranging from 0.32eV to 1.97eV. By mixing the halogen elements (Cl, Br, I) and changing the pnictide elements (Ge, Sn, Pb), we find the way to tune the band gap of the solar energy absorption materials. We propose several candidates for environmentally friendly solar energy absorbing materials with the absorption power as high as 1052 W/m$^2$.

(Received May 8, 2016; accepted August 9, 2017)

*Keywords:* Optical properties, Solar energy absorbing materials, Band gap tunable

## 1. Introduction

As the global demand for energy grows inexorably, solar energy attracts an increasing amount of attention owing to its abundant, clean, and renewable characteristics. The first generation crystalline silicon based solar cells reached a high efficiency, but they were limited by the low optical absorption coefficient and high cost of fabrication. Recently, the organic-inorganic hybrid pervoskites metal halides emerged as one kind of promising light-harvesting materials for the next generation solar cells due to their excellent properties, such as direct band gaps, large absorption coefficients and high carrier mobility [1-6]. Lee et al. [1] fabricated a low cost, solution-processable solar cell, based on the absorber $CH_3NH_3PbI_2Cl$, with the power conversion efficiency [PCE] as high as 10.9%. Soon after, Yuan [2] improved the PCE up to 13.56%, with low temperature Processing for $NH_2CH=NH_2PbI_3$. Burschka [3] improved the PCE up to 15%, with $CH_3NH_3PbI_3/TiO_2$ as the absorber. Beyond unitary halide organometal perovskites $CH_3NH_3PbX_3$ (X=Cl, Br, I), some mixed halide organometal perovskites $CH_3NH_3PbX_{3-y}X'_y$(X, X'=Cl, Br, I, $0<y<1$) caused people's attention. Because that such substitution can tune the band gap, which is important for the solar cell. Yang [4] partially substituted I atom with Cl atom in $MAPbI_3$ and improved the PCE up to 19.3% with high stability. Zhou et al. [5] found modest changes in the band gap, relative permittivity, and most other electronic properties with the rotation of $MA^{+1}$ ion in $CH_3NH_3PbI_3$. Shen [6] found the charge separation and recombination processes at the interfaces are particularly important for $CH_3NH_3PbClI_2$. Mosconi [7] studied the crystal and electronic structure of mixed halide organometal perovskites $CH_3NH_3PbI_2X$ (X=Cl, Br, I), and found that $CH_3NH_3PbI_2Cl$ had an absorption onset at ~800 nm, while $CH_3NH_3PbI_2Br$ below ~700 nm.

The organic ion $(CH_3NH_3)^{+1}$ in the organic-inorganic hybrid pervoskites halides can be replaced by $Cs^{+1}$ ion, constructing inorganic metal halides pervoskites. With first-principle calculations, Chang et al. [8] studied the structural and electronic properties of lead based $ABX_3$ compounds. Murtaza et al. [9] studied the structural and optoelectronic properties of cubic perovskites $CsPbX_3$ (X =Cl, Br, I). Lang et al. [10] studied the electronic and optical properties of cubic $ABX_3$ halide perovskites with first-principles. Their results showed that the band gap $E_g$ increases with the sizes of organic moleculars.

Although a lot of theoretical investigations about perovskite solar energy materials have been reported, no electronic structure calculation has performed on the mixed halide $ABX_3$ systems. In this work, we constructed a series of compounds $CsAX_2X'$(A=Ge, Sn, Pb; X,X'=Cl, Br, I), optimized their crystal structures and studied their electronic structures and optical properties by the first-principles calculations. By studying their band gap, optical absorption coefficient and Ideal Power Absorption Coefficient (IPAC), we find several possible solar energy absorbing materials: $CsGeI_2Br$, $CsGeI_3$, $CsGeBr_2I$, $CsGeBr_3$, $CsSnI_2Br$, $CsSnI_3$, and $CsSnI_2Cl$, with their IPAC as high as 1052 W/m$^2$.

## 2. Calculation methods

The structure optimization is performed by using the Vienna ab initio Simulation Package (VASP) [11-12]. The generalized gradient approximation (GGA) [13] formulated by Perdew-Burke-Ernzerhofer (PBE) [14] is employed for the exchange-correlation function. The electrical and optical properties were calculated based on the optimized structures with Wien2k package [15-16]. The modified Becke-Johnson (mBJ) [17] exchange-correlation potential was adopted for accurate band gaps and optical properties. The mBJ method successfully overcomes the problem of underestimating the band gap, since it considers the core electrons as fully relativistic and the valence electrons are treated semi-relativistically. The compounds $CsAX_2X'$ contain heavy elements Sn and Pb, which have large SOC effect. Previous researches indicated that there were greatly affected by the SOC effect [18-19] in the solar cell materials. So we include the SOC interaction by using the second-order-variation procedure in our calculation. To achieve the energy convergence, the basis function is expanded up to $R_{MT}\times K_{MAX}=7$, where $R_{MT}$ is the minimum radius of muffin-tin spheres and $K_{MAX}$ is the magnitude of the largest K vector in the plane wave expansion. 2000 k-points are used to obtain self-consistency, and 8000 k-points in the irreducible Brillouin zone (IBZ) are used in calculating the electronic and optical properties.

## 3. Results and discussion

### 3.1. Structural properties

$CsAX_3$ compounds have three phases under different temperatures, such as high temperature cubic [20], room temperature tetragonal [21], and low temperature orthorhombic structures [20]. In this work, we only consider the cubic structure with the Pm-3m (No.221) space group, as shown in Fig. 1(a). The structure of mixed metal halide $CsAX_2X'$ is shown in Fig. 1(b), where we replace one halogen atom X (in the c-axis) by the other kind of halogen element X'. The crystal symmetry of mixed metal halide is lowered to P4/mmm (No.123). The optimized lattice constants of cubic $CsAX_3$ and tetragonal $CsAX_2X'$ are presented in Table 1, which are in good agreement with the available experiment data [22-27]. The lattice constants of these crystals are shown in Fig. 2(a,b,c).

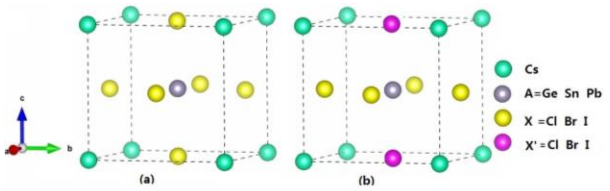


*Fig. 1. Crystal structure of (a) the cubic phase $CsAX_3$ and (b) the tetragonal phase $CsAX_2X'$*

From Table 1 and Fig. 2, we find the following rules: (1) the lattice constant a-axis (solid-line in Fig. 2a) of $CsACl_2X'$ increases from A=Ge, Sn, to Pb, while it hardly changes with substituting Cl ion by other halogen ions. (2) The lattice constant c-axis (dot-line in Fig. 2a) of $CsACl_2X'$ also increases from A=Ge, Sn, to Pb, and it quickly increases with substituting Cl ion by Br and I ions. This is because that we substituted one Cl ion in the c-axis with larger ions Br or I ions (see Fig. 1b). (3) For $CsAX_2X'$, when A and X' are fixed, their a-axis length increases from X=Cl to I, while the c-axis length hardly change. The lattice constant change rule can be understood by radius changes among A and the halogen ions.

*Table 1. The optimized lattice constant (in Å) of $CsAX_2X'$. The available experimental and theoretical results are shown in square brackets*

| | $CsACl_3$ | $CsACl_2Br$ | $CsACl_2I$ | $CsABr_2Cl$ | $CsABr_3$ | $CsABr_2I$ | $CsAI_2Cl$ | $CsAI_2Br$ | $CsAI_3$ |
|---|---|---|---|---|---|---|---|---|---|
| Ge | a=5.337<br>a=5.446[21] | a=b=5.348 | a=b=5.413 | a=b=5.616 | a=5.604<br>a=5.635[21] | a=b=5.631 | a=b=6.03 | a=b=6.003 | a=5.991<br>a=5.983[23] |
| | | c=5.60 | c=5.968 | c=5.336 | | c=5.97 | c=5.322 | c=5.603 | |
| Sn | a=5.618<br>a=5.56[17] | a=b=5.613 | a=b=5.642 | a=b=5.901 | a=5.885<br>a=5.807[22] | a=b=5.882 | a=b=6.321 | a=b=6.30 | a=6.273<br>a=6.219[20] |
| | | c=5.905 | c=6.319 | c=5.592 | | c=6.296 | c=5.569 | c=5.856 | |
| Pb | a=5.728<br>a=5.667[22] | a=b=5.725 | a=b=5.741 | a=b=6.03 | a=6.001<br>a=5.941[22] | a=b=6.002 | a=b=6.432 | a=b=6.413 | a=6.397<br>a=6.289[24] |
| | | c=6.027 | c=6.430 | c=5.697 | | c=6.420 | c=5.7 | c=5.981 | |

### 3.2. Electronic properties

Based on the optimized structures, we investigate the electronic structure of these compounds with the WIEN2k code. All of the $CsAX_2X'$ compounds have direct band gaps, shown in Fig. 2(d,e,f). Both the valence band maximum (VBM) and conduction-band minimum (CBM) located at the R point in Fig. 3(a,b,c). The calculated band gaps of $CsGeX_3$ were 1.34, 0.85, and 0.52 eV for X = Cl, Br, I, respectively, which are significantly smaller than the LDA results [28] (1.83 eV for $CsGeCl_3$ and 1.73 eV for $CsGeBr_3$). The band gaps of $CsSnX_3$ at the R-point were 1.24, 0.71, 0.32eV for the anion X = Cl, Br, I, respectively, and are agree with the theoretical calculate values of 1.19, 0.8, 0.49 eV [10] for X = Cl, Br. I. Previous studies indicate that both LDA and GGA calculations overestimated the band gap, while the SOC effect underestimated the band gap. We get the band gap of $CsPbX_3$ as 1.97, 1.31, and 0.73eV for Cl, Br, and I, respectively, which are smaller than the experimental results 3.0eV [29-30] for Cl, 2.25 eV [29-30] for Br [29] and 1.73 eV [31] for I, and are agree with the theoretical calculate values of 1.83, 1.32, 0.88 eV [10] for X = Cl, Br, I. So the mbj method can describe the electronic structure accurately and better than GGA or LDA.

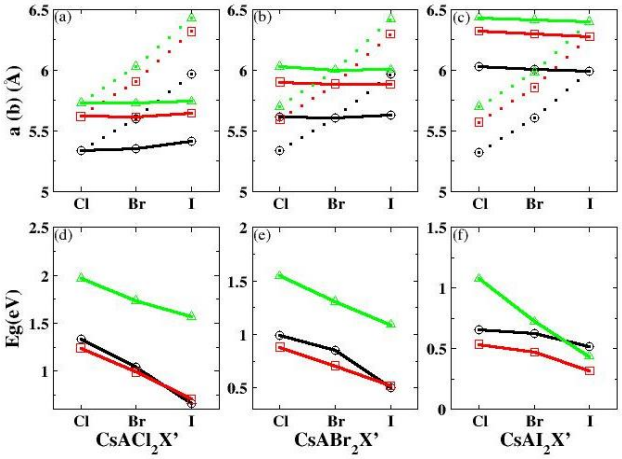


*Fig. 2. The lattice constant (a and c in Å) and band gap (Eg in eV) of CsAX2X'. In the figure (a), (b) and (c), the solid-line for a-axis, while the dot-line for c-axis. In all the figures, the black-circle, red-square, and green-triangle for A = Ge, Sn and Pb-based compound, respectively*

From Fig. 2(e,d,f), we can see that band gaps have a diminishing trend from Cl to I. In these compounds, the VBM is derived from the hybridized states between X-p and Pb-6s states, while the CBM is mostly derived from the Pb-6p states. Let's firstly focus on the band gaps of $CsAX_3$, with A changing from Ge to Pb and X ion being fixed. The band gap decreases from $CsGeX_3$ (Cl=1.24eV, Br=0.71eV, I=0.32eV), $CsSnX_3$ (Cl=1.24eV, Br=0.71eV, I=0.32eV), to $CsPbX_3$ (Cl=1.97eV, Br=1.31eV, I=0.73eV). The band gap decreasing is because of: (1) The ion radius of Ge and Sn are smaller than that of Pb, the band lengths of Ge-X and Sn-X are shorter than the Pd-X bond-length. The smaller bond-length, the stronger chemical bond, which increases the band gap between bonding state and anti-bonding states. This explanation can also answer the question why the band gap decreases from $CsACl_3$ to $CsAI_3$ (A-Cl bond length smaller than A-I bond length). (2) The band gap of the $CsAX_3$ comes from the energy level difference between A-nP states (CBM) and A-nS states (VBM). For $CsGeX_3$, such band gap comes from energy difference between 4p state and 4s state $E_{4p}$-$E_{4s}$, which is larger than the energy difference between 5p state and 5s state $E_{5p}$-$E_{5s}$ in the $CsSnX_3$ and $E_{6p}$-$E_{6s}$ in the $CsPbX_3$.

In order to explore the essential reason of the band gap change in the mixed halide compounds, we study the total and partial density of states (PDOS) of $CsAX_2X'$ compounds and present the result of $CsPbBr_2X'$(X'= Cl, Br, I) as an example in Fig. 3. The CBM is double degenerated in the pure compounds as shown in Fig. 3(b), while the CBM splits into Pb-$P_z$ and Pb-$P_{x+y}$ bands after substituting Br atom with Cl or I atom, shown in Fig. 3(a,c). Comparing the PDOS in Fig. 3, we find that the energy of Br-4p states higher than that of Cl-3p states (Fig. 3a), but lower than that of I-5p states (Fig. 3c). This explain why the band gap increases in the Cl-substituted compound and decreases in the I-substituted compound.

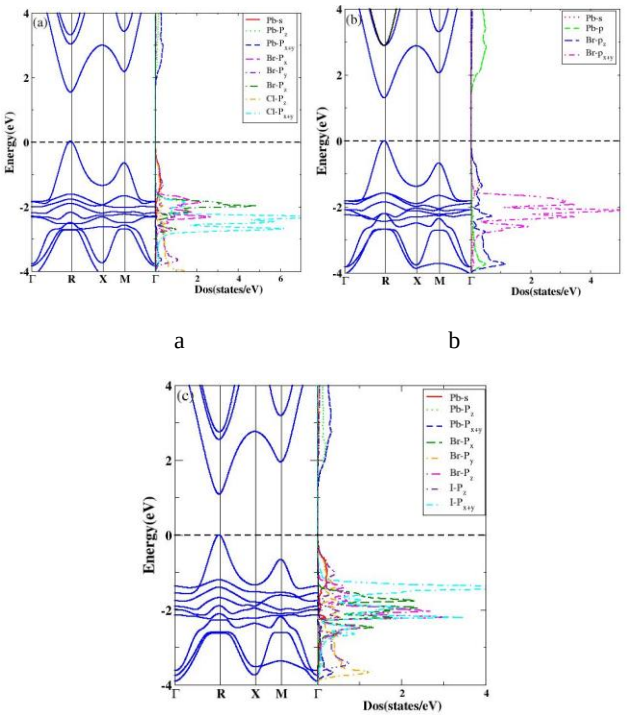


*Fig. 3. Band structure and projected density of states (PDOS) of $CsPbBr_2X'$ (X' =Cl, Br, and I) in figure (a), (b), and (c). The Fermi energy is at the VBM*

### 3.3. Optical properties

Semiconductors with direct band gap $E_g$ between 1.0 and 1.5 eV are generally well accepted to have the greatest potential in the application of high efficiency solar cells [32-34]. Our calculated band gaps in the Fig. 2 show that the compounds $CsACl_2X'$ may be more promising candidates for the solar cell absorbers. So, we present the absorption coefficient of all $CsAX_2X'$ compounds in the wavelength from 300 to1000 nm in Fig. 4. The absorption coefficients of Ge- and Pb-based compounds are significantly better than Sn-based compounds in the range of (300-600 nm). For all the compounds of $CsAX_2X'$, the absorption coefficient increases gradually with X' atom changing from Cl to I, when keeping the A and X atoms fixed. Some mixed halide compounds have larger absorption coefficient than that of pure ones, such as $CsSnCl_2I$, $CsSnCl_2Br$, $CsSnBr_2I$, $CsGeCl_2I$, $CsGeCl_2Br$, $CsGeBr_2I$, $CsPbCl_2I$, $CsPbCl_2Br$, $CsPbBr_2I$.

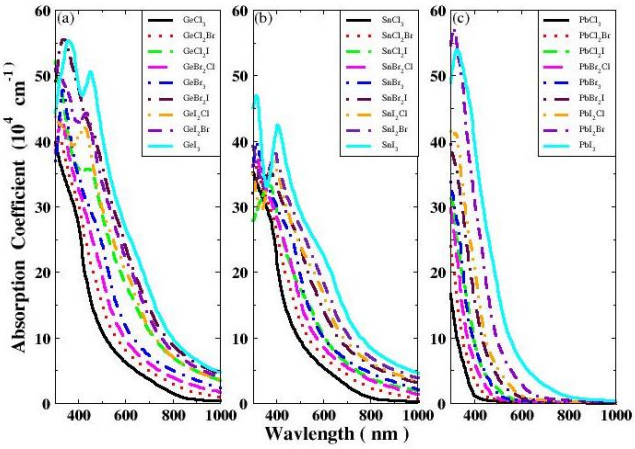


*Fig. 4. Absorption coefficient of $CsAX_2X'$, where the A ion is (a) Ge, (b) Sn and (c) Pb*

In Fig. 5, we present the Ideal Power Absorption Coefficient (IPAC), defined as $IPAC=I_0[1-e^{-2\alpha L}]$ [35], where the $I_0$ is the standard AM 1.5G solar spectrum [36], $\alpha$ is the absorption coefficient, L=50 nm is the thickness of the compound. The area enclosed by the IPAC curves and the abscissa x-axis is equal to the absorption power of the materials. We integrate the IPAC curves from 300 nm to 1000 nm. For the Ge-based compounds, $CsGeI_3$, $CsGeBr_2I$ and $CsGeBr_3$ have the largest absorption power ($1052W/m^2$). While the IPAC of $CsGeI_2Br$ and $CsGeI_2Cl$ compounds are a little smaller $1050W/m^2$, $1051W/m^2$, respectively. For the Sn-based compounds, $CsSnI_3$ has the largest absorption power ($1052W/m^2$). For the Pb-based compounds, $CsPbI_2Br$ has the largest ($878W/m^2$) absorption powers, but its IPAC is smaller than that of the Ge- and Sn-based compounds. From the IPAC, we expect the mixed halide compounds of $CsGeI_2Br$, $CsGeI_2Cl$, $CsGeBr_3$, $CsGeI_3$, $CsSnI_2Br$ and $CsSnI_3$ to be good candidates for solar energy absorption materials because of their large absorption powers and optimal band gaps.

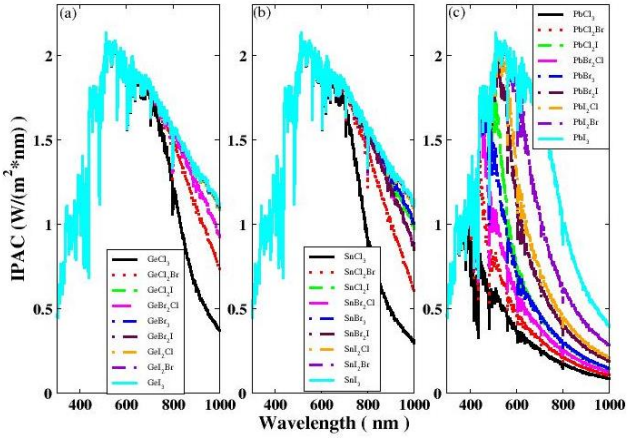


*Fig. 5. Ideal Power Absorption Coefficient(IPAC) of $CsAX_2X'$ under the standard AM 1.5G solar spectrum as a function of wavelength. Figure (a), (b) and (c) correspond to A=Ge, Sn and Pb, respectively*

## 4. Summary

In this work, we have studied the electronic structure and optical properties of the mixed halide perovskites $CsAX_2X'$(A=Ge, Sn, Pb; X, X'=Cl, Br, I) by using first-principles calculations. The optimized crystal structures are in good agreement with the experimental data. We find the way to tune the band gap of the solar energy absorption materials. We find several candidates for environmental-friendly solar energy absorption materials: $CsGeI_2Br$, $CsGeI_2Cl$, $CsGeBr_3$, $CsGeI_3$, $CsSnI_2Br$ and $CsSnI_3$ with their absorption powers as high as 1052 $W/m^2$.

### Acknowledgments

The authors acknowledge the support from NSF of China (No. 11274095, No. 10947001) and the high performance computing center of Henan Normal University.

### References

[1] M. M. Lee, J. Teuscher, T. Miyasaka, T. N. Murakami, H. J. Snaith, Science **338**(6107), 643 (2012).
[2] D. X. Yuan, A. Gorka, M. F. Xu, Z. K. Wang, L. S. Liao, Phys. Chem. Chem. Phys. **17**(30), 19745 (2015).
[3] J. Burschka, N. Pellet, S. J. Moon, R. Humphry

Baker, Nature **499**, 316 (2013).
[4] H. P. Zhou, Q. Chen, G Li, S. Luo, et al. Science **345**(6196), 542 (2014).
[5] Y. C. Zhou, F. Z. Huang, Y. B. Cheng, A. G -Weale, Phys. Chem. Chem. Phys. **17**(35), 22604 (2015).
[6] Q. Shen, Y. H. Ogomi, J. Chang, S. Tsukamoto, K. Kukihara, T. Oshima, N. Osada, K. Yoshino, K. Katayama, T. Toyoda, S. Hayase, Phys. Chem. Chem. Phys. **16**(37), 19984 (2014).
[7] E. Mosconi, A. Amat, Md. K. Nazeeruddin, M. Grätzel, F. D. Angelis, J. Phy. Chem. C. **117**(27), 13902 (2013).
[8] Y. H. Chang, C. H. Park, K. Matsuishi, Phys. Soc. **44**(4), 889 (2004).
[9] I. Khan, Iftikhar Ahmad, B. Amin, G Murtaza, Z. Ali, Physica B. **406**, 2509 (2011).
[10] L. Lang, J. H. Yang, J. H. Yang, H, R, Liu, H. J. Xiang, X. G Gong, Phys. Lett. A. **378**, 290 (2014).
[11] G Kresse, J. Hafner, Phys. Rev. B. **47**(1), 558 (1991).
[12] G Kresse, J. Hafner, Phys. Rev. B. **49**(20), 14251 (1994).
[13] G Kresse, D. Joubert, Phys. Rev. B. **59**(3), 1758 (1999).
[14] J. P. Perdew, K. Burke, M. Ernzerhof, Phys. Rev. Lett. **77**(18), 3865 (1996).
[15] P. Blaha, K. Schwarz, G K. H. Madsen, D. Kvasnicka, J. Luitz, WIEN2K: An Augmented Plane Wave and Local Orbitals Program for Calculating Crystal Properties, in: K. Schwarz (Ed.), Vienna University of Technology, Austria 2001.
[16] G H. Madsen, P. Blaha, K. Schwarz, E. Sjöstedt, L. Nordström, Phys. Rev. B **64**(19), 195134 (2001).
[17] F. Tran, P. Blaha, Phys. Rev. Lett. **102**(22), 226401 (2009).
[18] E. Mosconi, P. Umari, F. De Angelis, J. Mater. Chem. A **3**(17), 9208 (2015).
[19] M. G Ju, G X. Sun, Y. Zhao, W. Z. Liang, Phys. Chem. Chem. Phys. **17**(27), 17679 (2015).
[20] A. Poglitsch, D. Weber, J. Chem. Phys. **87**(11), 6373 (1987).
[21] Y. Kawamura, H. Mashiyama, K. Hasebe, Phys. Soc. **71**(7), 1694 (2002).
[22] J. Barrett, S. R. A. Bird, J. D. Donaldson, J. Silver, J. Chem. Soc. **A**(0), 3105 (1971).
[23] K. Yamada, S. Funabiki, H. Horimoto, T. Matsui, T. Okuda, S. Ichiba, Chem. Lett. **20**(5), 801 (1991).
[24] L. C. Tang, J. Y. Huang, C. S. Chang, M. H. Lee, L. Q. Liu, J. Phys.: Condens. Matter. **17**(47), 7275 (2005).
[25] L. Q. Jiang, J. K. Guo, H. B. Liu, M. Zhu, X. Zhou, P. Wu, C. H. Li, Phys. Chem. of Solids **67**(7), 1531 (2006).
[26] L. C. Tang, C. S. Chang, J. Y. Huang, Condens. Matter. **12**(43), 9129 (2000).
[27] D. M. Trots, S. V. Myagkota, Phys. Chem. of Solids **69**(10), 2520 (2008).
[28] L. Kang, D. M. Ramo, Z. H. Lin, P. D. Bristowe, J. G Qin, C. T. Chen, J. Mater. Chem. C **1**(44), 7363 (2013).
[29] K. Heidrich, W. Schafer, M. Schreiber, J. Sochtig, Phys. Rev. B **24**(10), 5642 (1981).
[30] Z. F. Liu, J. A. Peters, C. C. Stoumpos, M. Sebastian, B. W. Wessels, J. Im, A. J. Freeman, M. G Kanatzidis, Proc. of SPIE **8852**, 88520A (2013).
[31] P. P. Boix, S. Agarwala, T. M. Koh, N. Mathews, S. G Mhaisalkar, J. Phys. Chem. Lett. **6**(5), 898 (2015).
[32] A. Niv, Z. R. Abrams, M. Gharghi, C. Gladden, X. Zhang, Appl. Phys. Lett. **100**, 083901-1 (2012).
[33] C. Wadia, A. P. Alivisatos, D. M. Kammen, Environ. Sci. Technol. **43**(6), 2072 (2009).
[34] W. Shockley, H. J. Queisser, J. Appl. Phys. **32**(3), 510 (1961).
[35] X. Huang, T. R. Paudel, S. Dong, Phys. Rev. B. **92**(12), 125201 (2015).
[36] AM 1.5G http://rredc.nrel.gov/solar/spectra/am1.5/.

*Corresponding author: wangtao@htu.cn